



10.5281/zenodo.160965

## **EVALUATION OF THE TECHNOLOGICAL FEATURES OF LATE ROMAN COOKING WARE CLASSES FROM AKRAI (SYRACUSE, SICILY)**

**Germana Barone<sup>1</sup>, Roksana Chowaniec<sup>2</sup>, Simona Mangioni<sup>1</sup>, Paolo Mazzoleni<sup>1,\*</sup>,  
Simona Raneri<sup>1</sup>**

<sup>1</sup>*University of Catania, Department of Biol., Geol. and Environmental Sciences, C.so Italia 59, 95129 Catania - Italy*

<sup>2</sup>*University of Warsaw, Institute of Archeology, Krakowskie Przedmieście 26/28, PL 00-927, Warsaw, Poland*

**Received: 19/09/2016**

**Accepted: 11/10/2016**

*Corresponding author: Paolo Mazzoleni (pmazzol@unict.it)*

### **ABSTRACT**

In this work, a provenance and technological investigation on cooking-ware potteries from the ancient Greek -Roman town of Akrai (Palazzolo Acreide, Syracuse, Sicily) has proposed. A multi-methodological approach have been used to study the manufacture quality of analysed materials; in detail, petrographic, mineralogical, spectroscopic, chemical, porosimetric and micro-morphological analyses have been applied. The study provides fundamental contribute in archeological issues related to circulation in Sicily of cooking-ware productions during Late Roman Age; in fact, the obtained results allow to recognize in the site the presence of different well-known cooking-ware Roman productions, highlighting interesting questions about the technological and manufacture properties of this class of materials.

---

**KEYWORDS:** archaeometry, Akrai (Sicily); Cooking pottery; Late Roman; Pantelleria ware

---

## 1. INTRODUCTION

Cooking potteries represent a fundamental aspect in archaeological interpretation of the ancient culture being a common daily life element; for this reason, they are the most numerous record collected in the framework of archaeological excavations.

In general, potteries are high sensitive to the culture and commercial changes and often allow to highlight these variations. In fact, the circulation of different potteries production or, otherwise, the local production of vessels having peculiar typological and stylistic features are in many cases indicative of specific cultural processes. Therefore, the study of ancient ceramics can provide important information on social and political development of ancient centres, especially in cases of long occupancy and scarce historical sources. However, it is often difficult to obtain a complete knowledge of several aspects of materials only by macroscopic inspection and typological classification; thus, in some cases, a multifarious scientific approach is mandatory. In this sense, archaeometric investigations are fundamental in order to answer to the typical archaeological questions related to provenance (*e.g.*, geographical source of raw materials) and manufacture technology (*i.e.*, production process, decoration, firing temperature and condition, quality).

Among complex cultural processes that took place in antiquity, the *Romanization* of Sicily is one of the most debated in the archaeological literature. During this process several Sicilian centres were involved in a long-lasting cultural process responsible of the gradual vanishing of the Hellenistic elements and their substitution with the Roman ones.

The city of Akrai (Latin *Acrae*), located near the modern Palazzolo Acreide (Syracuse, Sicily), was particularly interested by the Romanization process in Sicily. This Greek colony founded in 664 B.C. was for a long time related to Syracuse. During the centuries, Akrai obtained some independence from the mother-colony, even though it had to pay tributes. Vast changes took place here during and after the Roman conquest of the Syracusan Kingdom 214–212 B.C.. The question how the town survived when Syracuse had broken down the peace with Rome and what actually happened here is taken under consideration in recent extensive studies (Chowaniec, 2015). In the framework of the excavations carried out in 2013 in the central, residential part of the ancient town (Chowaniec, 2013) by the Archaeological Mission of Institute of Archaeology University of Warsaw, in strictly cooperation with the Superintendence for Cultural Heritage of Syracuse, about 4400 ceramic shards have been yielded, largely represented by cooking ware type (about 870 fragments)

(Wicenciak, 2015). Thus, in consideration of the relevance of the site in the local scenario during the Roman period and the availability of a rich database on pottery production in Sicily and south Italy (Aquila *et al.* 2012; Barbera *et al.* 2013; Barone *et al.* 2005a; Barone *et al.* 2005b; Barone *et al.* 2009; Barone *et al.* 2012; Barone *et al.* 2014) a scientific project in collaboration with University of Catania, University of Warsaw and Superintendence of Cultural Heritage of Syracuse has been started.

## 2. MATERIAL AND METHODS

### 2.1 Materials

For this study, a selection of 38 cooking-ware fragments has been chosen for archaeometric analyses. The sampling have been carried out taking in consideration the different surface and clay body features of the shards and the stratigraphic distribution of ceramics, in order to have representative samples in term of dating and typology. In details, the analysed materials have been collected from stratigraphic units dating from the third century B.C. to the seventh A.D. The relative stratigraphic units (namely 1, 3, 4, 7, 8, 9, 10A, 11) could be described as levelling, rubble and abandonment layers. The selected fragments cover a limited shape repertoire (Figure 1), represented by pots and casseroles (CP), pans (P) and lids (L), some of them with specific manufacture features, *i.e.* coarse-grained clay paste, thick walls and heterogeneous surface, and sometimes burnished.

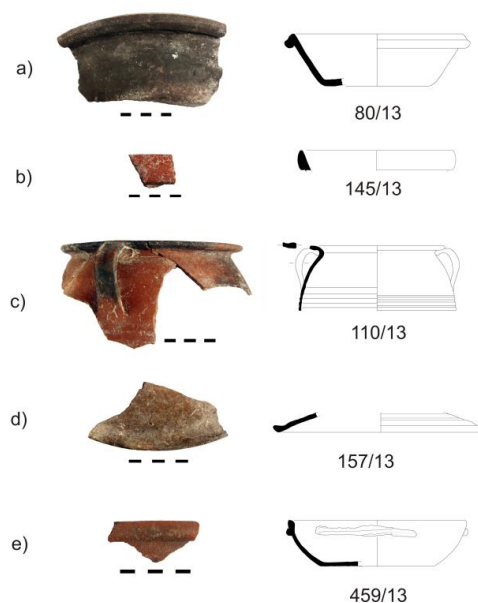


**Figure 1. Representative examples of cooking-ware fragments (a,b) pots, (c) casserole, (d) lid and (e) pan from Akrai (Palazzolo Acreide, prov. Syracuse, photo and drawing by Wicenciak Urszula)**

From archaeological and macroscopic point of view, three main archaeological fabriques can be recognized, namely fabrique 8, with large amount of white inclusions and micas (sub-fabrique 8a); fabrique 9, with white inclusions, and fabrique 10 with dark inclusions. Details on sample IDs, shape, ar-

chaological fabrique, provenance, dating of stratigraphic units (US), surface and bulk colour determined by Munsell color chart (Munsell Color Chart, 2000) are reported in Table 1, as well as the analyses performed for each sample.

**Table 1. List of cooking-ware fragments studied. Indication of sample IDs, shape, archaeological fabrique, provenance, dating of stratigraphic units (US), surface (S) and bulk (B) color determined by Munsell color chart (Munsell Color Chart, 2000) and analyses performed are reported: Optical Microscopy (OM), X Ray Diffraction (XRD);  $\mu$ Raman ( $\mu$ R); X Ray Fluorescence (XRF); Scanning Electron Microscopy (SEM); Mercury Intrusion Porosity (MIP).**

Sample ID	Shape	Arch. fabrique	Provenance	US dating	M.I.	OM	XRD	$\mu$ R	XRF	SEM	MIP
449/13	Lid (L2); rim	Fabrique 8	Trench I; US 1	End 3 AD-7 AD	S:5 YR 6/4	x	x		x	x	x
					B:7.5 YR 6/3						
450/13	Lid (L3); handle	Fabrique 8	Trench I; US 1	End 3 AD-7 AD	S:7.5 YR 6/4	x	x		x	x	x
					B:7.5 YR 4/4						
458/13	Pot (CP3); rim	Fabrique 9	Trench I; US 1	End 3 AD-7 AD	S:7.5 YR 5/4	x	x		x		
					B:GLE1 1 3 IN						
69/13	Jar	Fabrique 8	Trench I; US 3	End 3 AD-7 AD	S:2.5 YR 5/6	x	x	x	x		
					B:2.5 YR 5/8						
80/13	Pot (CP14)	Fabrique 8	Trench I; US3	End 3 AD-7 AD	S:7.5 YR 5/3	x	x		x		
					B:7.5 YR 4/4						
459/13	Pan(CP14); rim	Fabrique 9	Trench I; US 3	End 3 AD-7 AD	S:2.5 YR 5/6	x	x		x		
					B:7.5 YR 3/1 - 5 YR 4/6						
510/13	Lid (L4); rim	Fabrique 8	Trench I; US 3	End 3 AD-7 AD	S:7.5 YR 6/2	x	x	x	x		
					B:2.5 YR 5/6						
512/13	Lid (L3); rim	Fabrique 8	Trench I; US 3	End 3 AD-7 AD	S:2.5 YR 6/4	x	x		x		
					B:2.5 YR 6/3						
518/13	Jar; handle	Fabrique 8	Trench I; US 3	End 3 AD-7 AD	S:5 YR 5/6	x	x		x		
					B:7.5 YR 6/3						
520/13	Pot (CP2); rim	Fabrique 8	Trench I; US 3	End 3 AD-7 AD	S:7.5 YR 3/2	x	x		x		
					B:5 YR 5/6						
521/13	Pot (CP3); rim	Fabrique 9	Trench I; US3	End 3 AD-7 AD	S: 5 YR 6/6	x	x	x	x	x	x
					B: GLEY1 4/N						
561/13	Pot(CP18);rim	Fabrique 9	Trench I; US3	End 3 AD-7 AD	S:5 YR 5/6	x	x	x	x		
					B:GLEY1 2.5/N						
110/13	Casserole (CP6); rim	Fabrique 8a	Trench I; US4	2 AD-4 AD	S:7.5 YR 4/2	x	x		x		
					B:7.5 YR 3/4						
117/13	Pot (CP1); rim	Fabrique 8	Trench I; US4	2 AD-4 AD	S:5 YR 5/4- 7.5 YR 3/1	x	x		x		
					B:7.5 YR 3/3						
119/13	Pot (CP1); rim	Fabrique 8	Trench I; US4	2 AD-4 AD	S:7.5 YR 4/3-10 YR 3/1	x	x		x	x	x
					B:7.5 YR 4 /4						
121/13	Pot (CP7); rim	Fabrique 8	Trench I; US4	2 AD-4 AD	S:2.5 YR 5/6	x	x		x		
					B:2.5 YR 4/8						
143/13	Pot; bottom part	Fabrique 8a	Trench I; US4	2 AD-4 AD	S:2.5 YR 5/4	x	x		x	x	x
					B:7.5 YR 4/4						
144/13	Pot (CP2); rim	Fabrique 8	Trench I; US4	2 AD-4 AD	S:5 YR 4/3	x	x		x		
					B:7.5 YR 5/4						
145/13	Pot (CP2); rim	Fabrique 8	Trench I; US 4	2 AD-4 AD	S:2.5 YR 5/6	x	x	x	x	x	x
					B: GLEY1 4/N						
150/13	Lid (L1); rim	Fabrique 8	Trench I; US 4	2 AD-4 AD	S:10 YR 2/1	x	x		x		
					B:7.5 YR 3/4						
153/13	Lid (L2); rim	Fabrique 8	Trench I; US 4	2 AD-4 AD	S:7.5 YR 4/3	x	x		x		
					B:7.5 YR 3/4						
157/13	Lid (L2); rim	Fabrique 8	Trench I; US 4	2 AD-4 AD	S:7.5 YR 4/3	x	x		x		
					B:7.5 YR 3/4						
471/13	Pan (P1); rim	Fabrique 8a	Trench I; US 7	1 AD- half 5 AD	S:5 YR 4/4	x	x	x	x	x	x
					B:10 YR 4/2						
472/13	Pan (P1); rim	Fabrique 8a	Trench I; US 7	1 AD- half 5 AD	S:2.5 YR 4/6	x	x		x		
					B:5 YR 4/6						
478/13	Pot (CP1); rim	Fabrique 9	Trench I; US 7	1 AD- half 5 AD	S:7.5 YR 4/2- 5 YR 5/6	x	x		x	x	x
					B:5 YR 4/6						
479/13	Pan (P1); bottom part	Fabrique 8a	Trench I; US 7	1 AD- half 5 AD	S:5 YR 4/4	x	x	x	x	x	x
					B:7.5 YR 4/3-2.5Y 2.5/1						
480/13	Pot (CP2); rim	Fabrique 8	Trench I; US 7	1 AD- half 5 AD	S:5 YR 5/4	x	x		x		
					B:7.5 YR 4/4						
553/13	Pot (CP11); rim	Fabrique 8a	Trench I; US 7	1 AD- half 5 AD	S:2.5 YR 5/4	x	x	x	x		
					B:5 YR 4/6						
554/13	Pot; rim	Fabrique 8a	Trench I; US 7	1 AD- half 5 AD	S:5YR 2.5/1- 2.5 YR 4/4	x	x		x		
					B:5 YR 3/3						

502/13	Pot (CP1); rim	Fabrique 8	Trench I; US 8	1 AD- half 5 AD	S:5 YR 5/3	x	x		x		
					B:7.5 YR 5/1						
503/13	Pot (CP2); rim	Fabrique 8	Trench I; US 8	1 AD- half 5 AD	S:5 YR 4/3	x	x		x		
					B:5 YR 4/6						
495/13	Pan (P1); rim, body and handle	Fabrique 8.a	Trench I; US 9	3/2 BC-half 5 AD	S:5 YR 4/4	x	x		x		
					B:7.5 YR 3/4						
500/13	Pan (P1); rim	Fabrique 8a	Trench I; US 10a	3/2 BC-half 5 AD	S:2.5 YR 5/6	x	x		x		
					B:7.5 YR 3/4						
544/13	Pot (CP11); rim	Fabrique 8a	Trench I; US 10a	3/2 BC-half 5 AD	S: 2.5 YR 5/6	x	x		x		
					B:5 YR 4/6						
545/13	Pot (CP11); rim	Fabrique 8a	Trench I; US 10a	3/2 BC-half 5 AD	S:10 R 5/6	x	x		x		
					B:2.5 YR 5/8						
546/13	Pot (CP11); body	Fabrique 8a	Trench I; US 10a	3/2 BC-half 5 AD	S:5 YR 5/6	x	x	x	x		
					B:5 YR 4/6						
562/13	Pot; rim	Fabrique 8a	Trench I; US 10a	3/2 BC-half 5 AD	S:2.5 YR 5/4	x	x		x		
					B:7.5 YR 3/4						
558/13	Pot; bottom part	Fabrique 8a	Trench I; US 11	3/2 BC-3 AD	S:2.5 YR 5/6	x	x		x		
					B:5 YR 4/6						

## 2.2 Methods

Thin section analyses have been carried out following the Whitbread classification (Whitbread, 1995) that allows to highlight inclusions and groundmass features.

Information on mineralogical phases have been obtained by X-ray diffraction analysis (XRD) performed by using a SIEMENS D 5000 with Cu-K $\alpha$  radiation and an Ni filter. Randomly oriented powders were scanned from 2° to 45° 2 $\theta$ , with a 0.02° 2 $\theta$  step size with a counting time of 2 s per step. The tube current and the voltage were 30 mA and 40 kV, respectively.

In addition, the mineralogical composition of the matrix has been investigated by micro-Raman spectroscopy; in particular, spectra have been acquired on polished thin sections with a Raman Jasco NRS-3100 apparatus, equipped with a microscope with 10x, 20x and 100x objectives and two laser excitation source at 532 and 785 nm. For this study, the 785 nm line has been used; laser power has been controlled by means of a series of density filters, to avoid heating effects; depth resolution was set to few micrometers by means of a confocal hole; finally, the system has been calibrated using the 520.7 cm<sup>-1</sup> Raman band of silicon before each experimental session.

Chemical analyses for major oxides and trace elements have been performed by X-ray fluorescence spectrometry (using a Philips PW 2404/00) on powder-pressed pellets. Quantitative analysis was carried out using a calibration line based on 45 international rock standards. The limits of detection (LOD) were as follows: SiO<sub>2</sub> = 1 wt%, TiO<sub>2</sub> = 0.01 wt%, Al<sub>2</sub>O<sub>3</sub> = 0.1 wt%, Fe<sub>2</sub>O<sub>3</sub> = 0.05 wt%, MnO = 0.01 wt%, MgO = 0.02 wt%, CaO = 0.05 wt%, Na<sub>2</sub>O = 0.01 wt%, K<sub>2</sub>O = 0.05 wt%, P<sub>2</sub>O<sub>5</sub> = 0.01 wt%, V = 10 ppm, Cr = 5 ppm, Ni = 5 ppm, Zn = 15 ppm, Rb = 5 ppm, Sr = 10 ppm, Y = 3 ppm, Zr = 20 ppm, Nb = 2 ppm, Ba = 30 ppm, La = 5 ppm, Ce = 10 ppm, Pb = 7 ppm, Th = 3 ppm. The precision was monitored by routinely

running a well-investigated in-house standard (obsidian), while accuracy was evaluated using international standards compositionally similar to the samples analysed (SCO1 and SGR1). The average relative standard deviations (RSD) were less than 5%. Finally, the accuracy was evaluated using an international standard (SGR1) that is compositionally similar to the analysed samples. The accuracy was good for major elements (<3%), except for MnO, and for trace elements (5%).

Chemical data have been treated with the statistical method mainly based on the log-ratio technique introduced by Aitchison (Aitchison, 1986) and employed in order to avoid the constant sum problem; the centred log-ratio transformation (clr) of data is applied as follows:  $x \in SD \rightarrow y = \ln(xD / gD(x)) \in RD$  where  $x$  is the vector of the D elemental compositions,  $y$  is the vector of the log-transformed compositions,  $xD = (x_1, x_2, \dots, x_D)$  and  $gD(x) = (x_1 \cdot x_2 \cdot \dots \cdot x_D)^{1/D}$ . This operation transforms the raw data from their constrained sample space, the simplex  $S_d(d = D - 1)$ , into the real space  $R_d$ , in which parametric statistical methods can be applied to the transformed data. Subsequently, the clr-transformed data set was explored by biplots, a graphical representation of variables and cases projected on to principal component planes. Both the clr-transformation and the biplot calculations were obtained by using CoDaPack (Thio-Henestrosa and Martin Fernandez, 2005) a compositional software that implements the basic methods of analysis of compositional data based on log-ratios.

Information on the degree of vitrification reached by the samples during firing have been obtained by micro-morphological analysis using a scanning electron microscopy (SEM); measurements have been performed using a Tescan Vega LMU scanning electron microscope, equipped with an EDAX NeptunexM4-60 micro-analyzer, characterized by an ultra-thin Be window. Measurements were carried out on small fragments drawn from the samples and at

tached to an aluminum stub with double-sided tape and coated in carbon, with 20 kV accelerating voltage and 0.2 nA beam current.

Finally, data on distribution of the pores have been obtained by mercury intrusion porosimetric analyses performed with a Thermoquest Pascal 240 macropore unit in order to explore a porosity range  $\sim 0.0074 \mu\text{m} < r < \sim 15 \mu\text{m}$  ( $r$  being the radius of the pores) and by a Thermoquest Pascal 140 porosimeter instrument in order to investigate a porosity range from  $\sim 3.8 \mu\text{m} < r < \sim 116 \mu\text{m}$ .

### 3. RESULTS

#### 3.1 Petrographic and mineralogical data

Thin section analyses allow us to identify three petrographic fabrics, namely Fabric A, Fabric B and Fabric C. Samples of Fabric A (specimens 69/13, 80/13, 117/13, 119/13, 121/13, 144/13, 145/13, 150/13, 449/13, 478/13, 480/13, 502/13, 503/13, 510/13, 512/13, 518/13, 520/13, 554/13) are characterized by coarse grain size, heterogeneous groundmass and volcanic inclusions with anorthoclase (Figure 2(a),

aegirine (Fig. 2(b)) and aenigmatite (Fig. 2(c)). In detail, the microstructure consists mainly of sub-spherical voids and scarce planar voids, without preferred orientation and exhibiting open-double spaced spatial distribution. The groundmass is heterogeneous in color, ranging from reddish-brown to dark-brown. It is characterized by high to medium-high or locally low birefringence. The inclusions have a single space distribution and polymodal grain size (from 0.5 to 2 mm). The inclusions-to-groundmass ratio is about 40:60. The coarser grain inclusions are represented by anorthoclase, aegirine, volcanic glass fragments and rare aenigmatite with prevalently sub-angular shape, while the finer ones are mainly anorthoclase and quartz. Finally, brownish-black amorphous phases are present. Fabric B (specimens 110/13, 143/13, 153/13, 157/13, 450/13, 471/13, 472/13, 479/13, 495/13, 500/13, 544/13, 545/13, 546/13, 553/13, 558/13, 562/13) is characterized by medium grain size, micaceous groundmass and metamorphic rock fragments inclusions (Fig. 2(d, e).

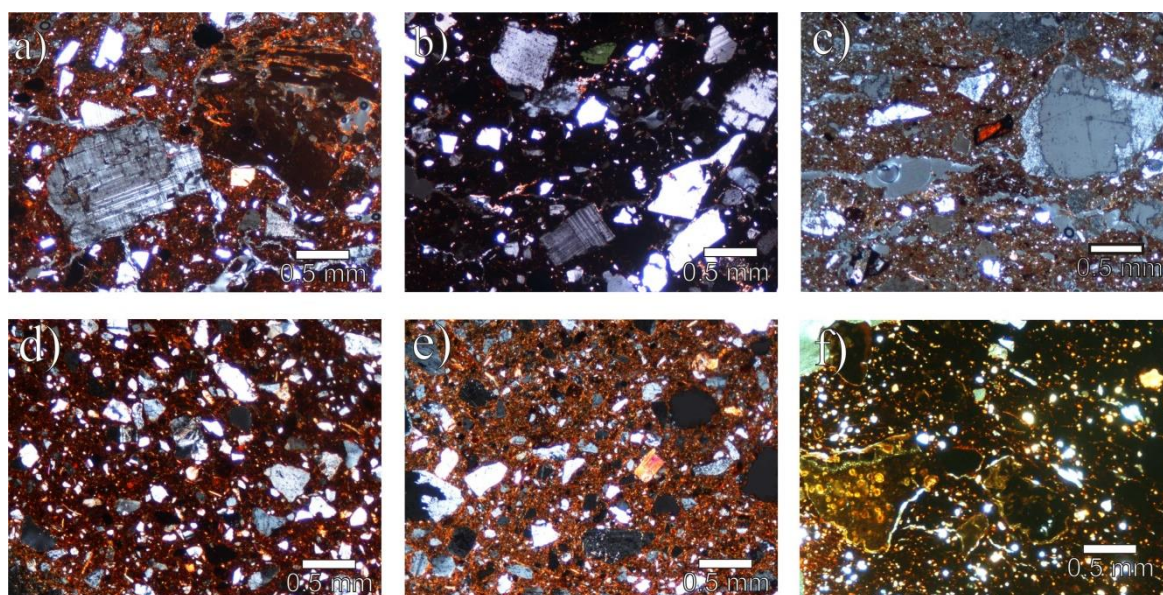


**Figure 2.** Microphotographs of representative samples for each petrographic fabric identified. Fabric A: a) microcline and volcanic glass in 80/13, b) aegirine in 117/13 and c) aenigmatite in 510/13 samples. Fabric B: metamorphic rock fragments and micaceous groundmass in samples d) 472/13 and e) 500/13; Fabric C: volcanic glass inclusions and zeolite in samples 459/13.

In particular, the voids microstructure is characterized by sub-spherical voids, channels and planar voids, the latter ones slightly oriented; voids spatial distribution is mainly doubled spaced. The groundmass is micaceous and very homogeneous with medium birefringence and reddish-brown color. The grain size distribution of inclusions is quite unimodal; mineralogical composition of inclusion is due to quartz, metamorphic rock fragments (polycrystalline quartz, phyllite and schist), biotite, scarce plagioclase

and rare amphibole, sub-angular in shape and sub-millimetric in dimension (average grain size about 0.25-0.5 mm); the inclusions-to-groundmass ratio is about 30:70. Scarce reddish-black amorphous phases are present. Finally, Fabric C (specimens 458/13, 459/13, 521/13 and 561/13) is characterized by very heterogeneous groundmass and volcanic glass inclusions (Figure 1(f)). In detail, microstructure is due to scarce sub-spherical voids and abundant planar voids, the latter ones partially oriented (except in



sample 521/13) and single spaced. The groundmass is heterogeneous in color and characterized by reddish-brown/brownish-black color; moreover, birefringence is absent. Inclusions, polymodal in grain size distribution, are mainly made by volcanic glass in the coarser fraction; the finer one is characterized by dominant quartz and frequent olivine and pyroxene, widely altered; rare inclusions of zeolites are also present. The inclusions-to-groundmass ratio is about 10:90. Finally, reddish oxides are abundant and dispersed in the groundmass.

In order to obtain deeper information on mineralogical composition of samples and esteem firing

temperature, semi-quantitative data of the X-ray patterns have been analysed (Table 2). According to literature (Maggetti, 1982; Riccardi *et al.* 1999), mineralogical composition of samples is able to supply information on firing condition achieved in manufacture process on the basis of newly formed minerals growth by chemical reactions between minerals in the clay; in particular, in Ca-rich clays, the presence of Ca-silicates phases as gehlenite, anorthite and diopside is indicative of high firing temperature (about 850-900 °C); of course, neither anorthite nor diopside can be used for temperature esteem when related to tempers composition.

**Table 2. Petrographic and mineralogical data of the studied samples. Birefringence: +++ = high; ++ = medium; + = low or absent birefringence; Qz = Quartz; Ano = Anorthoclase; Mc = Microcline; Gh = gehlenite; An = Anorthite; Di = diopside; Hem = Hematite; Zeo = zeolite; CM = Clay Minerals. The number of (+) is related to the mineralogical phase abundance: +++ = abundant; ++ = present; + = scarce/rare; - = absent.**

		ID	Birefringence	Qz	Ano	Mc	Gh	An	Di	Hem	Zeo	CM
FABRIC A	Heterogeneous groundmass; volcanic inclusions (glass and rock fragments) with aegirine, anorthoclase and aenigmatite	69/13	++	+	+++	-	-	-	+	++	-	-
		80/13	++/	+	+++	-	-	-	+	++	-	-
		117/13	++/+	+	+++	-	-	-	+	++	-	+
		119/13	+++	+	+++	-	-	-	+	++	-	+
		121/13	-	+	+++	-	-	-	+	++	-	+
		144/13	-	+	+++	-	-	-	+	+	-	-
		145/13	++	+	+++	-	-	-	+	+	-	-
		150/13	++/+	++	+++	-	-	-	+	+	-	-
		449/13	++	+	+++	-	-	-	+	+	-	-
		478/13	++	+	+++	-	-	-	+	+	-	-
		480/13	+++	-	+++	-	-	-	+	++	-	-
		502/13	+++	-	+++	-	-	-	+	++	-	-
		503/13	+++	+	+++	-	-	-	+	+	-	-
		510/13	-	+	+++	-	-	-	++	+	-	-
		512/13	++	+	+++	-	-	-	++	++	-	-
		518/13	++	+	+++	-	-	-	++	++	-	-
		520/13	+++	+	+++	-	-	-	++	++	-	-
554/13	++/+	+	+++	-	-	-	+	++	-	-		
FABRIC B	Micaceous groundmass with metamorphic rock fragments inclusions	110/13	++	+++	-	+	-	++	++	+	++	-
		143/13	-	+++	-	+	-	++	+	+	-	-
		153/13	+++	+++	-	+	+	+	+	+	+	-
		157/13	+++	+++	-	+	-	++	-	-	+	-
		450/13	-	+++	-	+	-	++	+	-	-	-
		471/13	+++	+++	-	+	-	++	-	-	++	-
		472/13	+++	+++	-	-	-	++	+	-	+	-
		479/13	+++	+++	-	+	-	++	+	-	++	-
		487/13	-	+++	-	-	+	+	+	-	-	-
		495/13	-	+++	-	+	-	++	+	-	-	-
		500/13	+++	+++	-	+	+	+	+	-	+	-
		544/13	-	+++	-	+	-	+++	+	-	-	-
		545/13	-	+++	-	+	+	++	+	+	-	-
		546/13	++	+++	-	-	+	++	+	+	+	-
553/13	+++	+++	-	-	-	++	-	+	++	-		
558/13	-	+++	-	-	-	++	+	+	-	-		
562/13	+++	+++	-	+	-	++	+	+	+	-		
FABRIC C	Heterogeneous groundmass with volcanic glass inclusions, zeolite and oxides	458/13	-	++	-	-	+	+	-	+	-	++
		459/13	-	+++	-	+	-	++	-	++	-	-
		521/13	-	+++	-	-	++	+	-	+	+	+
		561/13	-	+++	-	-	+	+	+	-	-	-

*Table 3. Chemical composition of studied samples. Major elements are reported in wt%; minor elements are in ppm. The chemical data reported have been recalculated to 100% on volatile-free basis.*

Sample ID	Fabric	SiO <sub>2</sub>	TiO <sub>2</sub>	Al <sub>2</sub> O <sub>3</sub>	Fe <sub>2</sub> O <sub>3</sub>	MnO	MgO	CaO	Na <sub>2</sub> O	K <sub>2</sub> O	P <sub>2</sub> O <sub>5</sub>	Sr	V	Cr	Co	Ni	Zn	Rb	Y	Zr	Nb	Ba	La	Ce	Pb	Th
69/13	Fabric A	61.22	1.22	19.96	8.91	0.09	0.33	1.06	4.03	2.99	0.20	206	b.d.l.	11	1	9	156	36	59	848	174	1290	105	208	9	17
80/13	Fabric A	58.20	1.07	21.65	9.37	0.21	0.52	2.73	3.63	2.40	0.22	315	b.d.l.	4	3	10	167	39	78	852	176	996	107	265	13	14
117/13	Fabric A	60.41	1.10	20.20	8.81	0.17	0.68	2.17	3.59	2.67	0.21	255	b.d.l.	4	3	7	149	34	55	660	136	1206	78	179	5	14
119/13	Fabric A	58.77	1.16	21.98	8.26	0.18	0.54	2.79	3.36	2.55	0.41	351	b.d.l.	3	0	8	155	37	65	770	163	1099	103	224	7	13
145/13	Fabric A	60.77	1.49	18.53	9.72	0.11	0.43	1.03	4.33	3.47	0.11	136	b.d.l.	1	0	10	160	43	56	608	126	1242	99	190	13	13
150/13	Fabric A	56.46	1.64	22.40	10.47	0.21	1.26	3.21	2.01	1.75	0.60	301	b.d.l.	7	3	10	190	31	71	595	121	1625	105	222	5	12
449/13	Fabric A	57.60	1.29	22.65	10.50	0.22	0.44	1.43	3.09	2.49	0.28	255	b.d.l.	3	1	8	307	55	90	1241	258	912	134	323	12	24
478/13	Fabric A	60.22	0.93	19.71	9.19	0.20	0.55	1.81	4.07	3.16	0.16	217	b.d.l.	11	1	9	184	61	76	1016	195	913	95	252	5	20
480/13	Fabric A	60.29	1.04	21.25	8.61	0.14	0.54	1.90	3.56	2.48	0.20	247	b.d.l.	2	0	10	146	30	45	645	128	1121	80	173	4	13
502/13	Fabric A	57.68	1.18	22.82	9.15	0.15	0.44	2.24	3.53	2.31	0.49	356	b.d.l.	8	3	7	144	26	68	796	163	1332	102	229	7	18
503/13	Fabric A	59.38	1.06	20.60	9.48	0.21	0.57	2.30	3.50	2.66	0.24	327	6	18	3	11	139	56	58	669	138	1223	81	210	17	14
512/13	Fabric A	58.72	1.23	23.25	8.89	0.15	0.45	1.56	3.03	2.49	0.24	231	b.d.l.	5	0	9	149	33	74	913	189	1193	114	233	5	20
518/13	Fabric A	58.39	1.36	23.08	9.18	0.17	0.68	1.30	3.16	2.41	0.28	218	b.d.l.	4	8	8	162	26	67	880	177	1354	123	266	7	18
520/13	Fabric A	58.32	1.15	21.92	9.50	0.15	0.41	2.10	3.62	2.56	0.28	316	b.d.l.	9	2	18	148	37	60	791	156	1211	88	206	8	14
554/13	Fabric A	59.06	1.02	19.94	10.65	0.25	0.67	1.08	3.80	3.45	0.08	93	18	27	5	21	172	79	58	728	141	844	102	273	12	17
121/13	Fabric A	59.46	1.07	20.12	10.86	0.19	0.53	1.36	3.66	2.64	0.12	209	b.d.l.	3	3	7	236	52	115	1314	259	893	152	358	13	27
144/13	Fabric A	59.19	1.15	21.83	9.73	0.18	0.93	1.98	2.61	2.03	0.37	239	b.d.l.	3	0	9	216	37	78	880	179	859	111	267	17	17
510/13	Fabric A	60.03	1.30	22.06	6.32	0.09	0.28	2.38	3.23	3.38	0.92	393	b.d.l.	4	1	10	146	41	69	841	176	1399	109	250	11	14
110/13	Fabric B	60.68	1.04	20.43	9.08	0.20	1.49	2.62	1.49	2.61	0.36	369	132	68	18	33	113	129	34	217	24	654	43	94	36	15
143/13	Fabric B	60.13	1.17	20.91	9.93	0.19	1.48	1.67	1.57	2.73	0.22	243	167	77	26	42	118	130	32	252	26	604	46	110	37	17
153/13	Fabric B	65.00	0.91	17.32	7.76	0.11	1.54	2.63	1.78	2.67	0.26	347	116	58	20	36	101	118	24	206	20	564	34	92	43	14
157/13	Fabric B	63.00	0.94	19.02	8.35	0.14	1.51	2.80	1.54	2.42	0.27	316	128	63	17	39	112	102	20	155	13	573	46	89	30	13
450/13	Fabric B	64.24	0.91	18.83	7.44	0.12	1.47	2.26	1.59	2.96	0.19	321	109	61	17	31	89	132	21	195	16	591	41	65	44	11
471/13	Fabric B	62.60	0.97	18.83	7.98	0.16	1.53	3.77	1.60	2.27	0.28	351	116	65	21	33	92	108	21	173	14	552	41	102	37	14
472/13	Fabric B	62.95	0.95	18.28	7.58	0.13	1.48	2.83	1.79	3.72	0.30	420	106	69	18	33	98	121	19	187	15	615	27	73	35	13
479/13	Fabric B	64.84	0.91	18.24	7.54	0.14	1.30	2.17	1.80	2.76	0.32	293	114	56	23	31	91	122	30	230	20	563	42	81	30	16
495/13	Fabric B	63.93	0.93	18.64	7.91	0.13	1.48	2.55	1.50	2.66	0.27	324	127	64	22	36	99	124	26	188	18	601	38	80	44	14
500/13	Fabric B	64.49	0.91	18.14	7.70	0.11	1.39	2.71	1.59	2.70	0.26	317	107	63	25	32	91	124	21	166	14	570	35	82	27	13
544/13	Fabric B	62.35	1.01	19.79	8.56	0.16	1.48	1.60	1.75	3.03	0.26	253	135	65	19	32	113	147	34	256	27	612	48	106	35	18
545/13	Fabric B	61.55	1.18	19.45	9.87	0.13	1.53	1.26	1.65	3.22	0.16	194	147	79	15	38	115	147	37	233	24	642	58	115	37	16
546/13	Fabric B	62.52	1.01	19.41	8.68	0.16	1.41	1.64	1.82	3.09	0.27	232	135	67	16	34	113	130	28	225	19	627	54	108	35	14
553/13	Fabric B	62.33	1.06	19.74	8.91	0.17	1.33	2.13	1.47	2.55	0.30	302	123	70	21	35	105	125	24	190	16	614	45	107	37	13
558/13	Fabric B	63.64	0.95	19.55	8.12	0.15	1.19	2.14	1.41	2.57	0.28	331	104	61	20	30	95	127	24	194	17	596	44	97	30	14
562/13	Fabric B	61.59	1.02	20.22	8.88	0.17	1.55	2.25	1.51	2.52	0.28	355	121	73	15	37	105	135	31	217	23	617	44	98	35	15
458/13	Fabric C	53.36	2.84	17.23	17.33	0.21	2.69	2.15	0.54	0.43	0.25	175	207	325	65	177	98	18	45	273	39	451	43	112	11	8
459/13	Fabric C	57.95	3.04	17.24	15.03	0.23	2.45	2.51	0.79	0.55	0.22	212	191	287	50	128	97	18	35	321	38	429	49	122	14	10
521/13	Fabric C	54.18	3.01	20.13	15.29	0.45	3.04	2.37	0.73	0.56	0.25	223	225	297	90	146	96	27	51	373	53	632	64	184	16	14
561/13	Fabric C	56.42	2.70	16.26	16.09	0.15	2.80	3.98	0.58	0.46	0.56	390	167	386	33	191	121	26	76	272	48	431	77	137	14	9

In the case of cooking-wares, usually made with poor-Ca clay materials, the absence of carbonates doesn't allow the formation of Ca-silicate and changes are mainly related to textural features, with the only transformation of low-T phases in high T-phases. However, some minerals can be used as temperature indicators, as phyllosilicates and hematite (Cultrone *et al.* 2001). In fact, in XRD patterns of Ca-poor clay materials, a gradual reduction of peaks intensity of phyllosilicate due to dehydroxilation of clay minerals and an increase of peaks related to hematite can be observed with the increasing of fired temperature. In the cases of studied materials, in samples belonging to Fabric A the most abundant phases are represented by anorthoclase, diopside and quartz, according to the petrographic observations; moreover, calcite is absent and the presence of hematite suggests medium-low firing temperature, in agreement with the medium-high birefringence observed in thin section.

Samples of Fabric B are characterized mainly by quartz, anorthite and diopside, with really small amount of hematite. Calcite is absent; however, the presence of really small amount of ghelentite in some samples could suggest the presence of low level of calcite in the raw clay sediment and the occurrence of reactions at temperatures above 800 °C. These observations match with the petrographic data related to medium birefringence of the matrix. In addition, the occasional presence of zeolites could be related to post-burial alteration.

Finally, in the case of Fabric C samples, beside quartz, clay minerals, hematite and zeolites, the mineralogical composition highlights the presence of small amount of anorthite, diopside and ghelentite, suggesting the achievement of medium-high firing temperature and small amount of calcite in the employed raw materials ( $T_{max} > 850$  °C).

The mineralogical composition of the matrix has been in-depth investigated by spectroscopic analyses; in detail, micro-Raman spectra have been collected in the range 200 - 1800  $cm^{-1}$  from different spots on polished thin sections. Data have been acquired on representative samples of petrographic fabrics previously identified; in detail, spectra have been collected on specimens 69/13, 145/13 and 510/13 belonging to Fabric A, on 471/13, 479/13, 553/13 and 546/13 classified in Fabric B and on samples 521/13 and 561/13 for Fabric C (Figure 3). In the case of Fabric A samples, Raman bands centered at 227, 293, 411 and 613  $cm^{-1}$  and related to hematite have been observed; in addition, a weak band related to feldspar (centered at about 511  $cm^{-1}$ ) has been also detected. In samples belonging to Fabric B the main mineralogical phases detected include quartz and hematite; in detail, beside the typical

Raman bands due to hematite, the strong band at 464  $cm^{-1}$  due to quartz has been detected. Finally, in the Raman spectra collected on Fabric C samples, intense bands centered at about 1345 and 1605  $cm^{-1}$  and attributable to amorphous carbon have been observed.

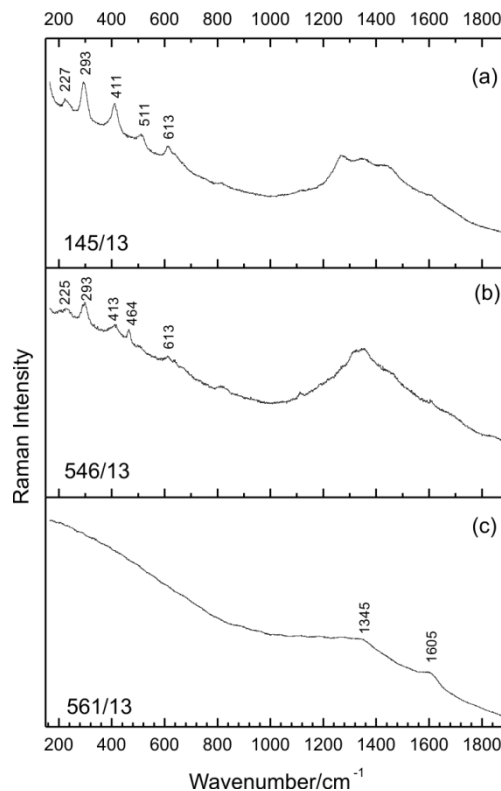


Figure 3. Micro-Raman spectra collected on the matrix of representative samples belonging to Fabric A (451/13), Fabric B (546/13) and Fabric C (561/13) are shown, as examples.

### 3.2 Chemical composition

The statements on composition of clays assumed from ware typology and mineralogical composition are confirmed by chemical data; in fact, level of CaO is lower than 6% (poor-Ca clays) in all samples; however, differences in chemical composition among the petrographic fabric can be recognized (Table 3); referring to major elements, samples belonging to Fabric A are characterized by higher levels of  $Al_2O_3$ ,  $Na_2O$  and lower MgO than Fabric B. Otherwise, Fabric C samples are characterized by definitely higher high levels of  $Fe_2O_3$  (~15%),  $TiO_2$  (~3 wt%) and MgO (~2.5 wt%) than other fabrics. About minor and trace elements, Fabric A potteries are characterized by really low level in V and Cr (in many cases lower than the detection limits) and high level in Nb (> 100 ppm) and Zr (> 600 ppm), while samples of fabric B are distinguished for  $Rb > 80$  ppm. Finally, samples of Fabric C are distinguished



for higher levels of Cr (~ 300 ppm), Co (~ 60 ppm) and Ni (~ 150 ppm) than all other samples.

### 3.3 Textural and structural features

Micro-morphological observations on representative samples for each petrographic fabric have been carried out by using scanning electron microscope (SEM) in order to provide information on the degree of vitrification reached during firing (Maniatis and Tite, 1981). By observing the images collected on the rough surface of samples it is possible to assess an absence of vitrification for Fabrics A (Figure 4a) and B (Figure 4b) samples and an initial stage of vitrification for samples of Fabric C (Figure 4c). In details,

the formers show an aggregate of flaky clay particles in which tempers are dispersed; low amount of pores, mainly not connected, are also visible. Otherwise, in samples of Fabric C a high concentration of fine bloating pores is visible, associated with the presence of abundant planar voids.

In order to deepen investigate aspects related to pore network arrangement of studied materials, mercury intrusion porosimetry (MIP) measurements have been carried out. The collected data highlight different structural features for samples belonging to the three groups recognized by previous analyses.

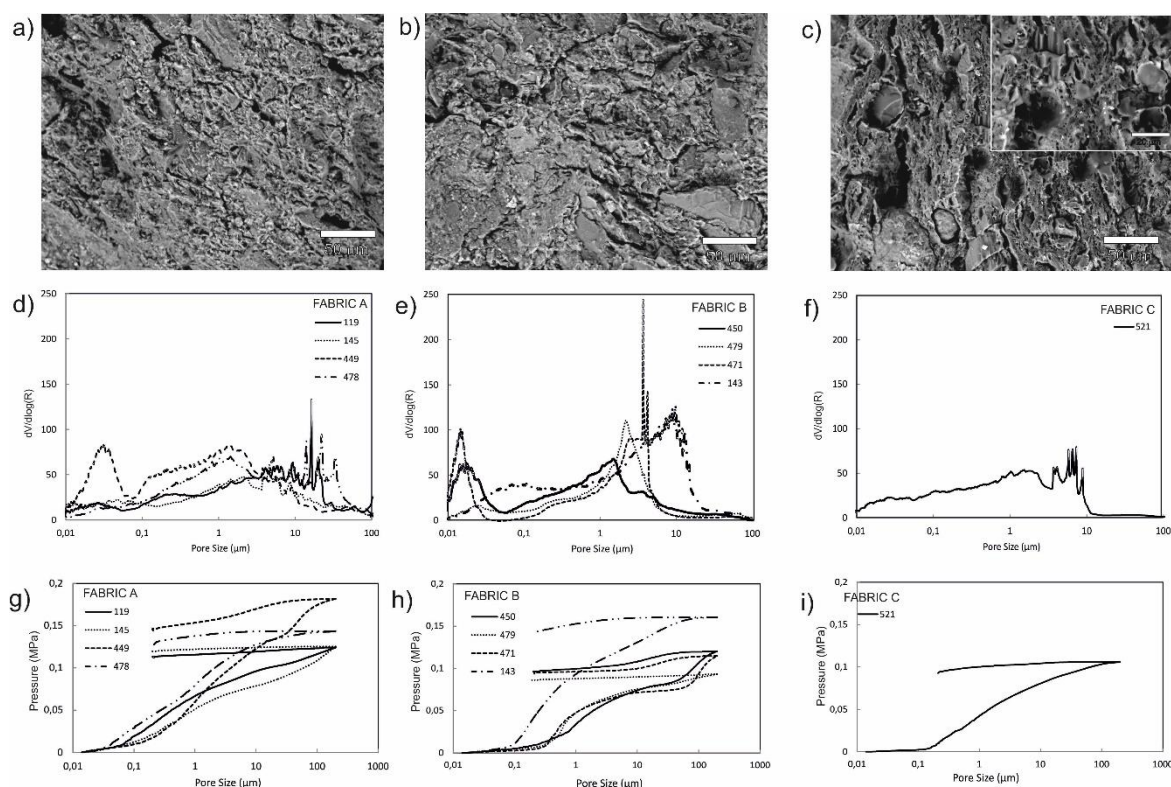


**Figure 4.** Data about technological features (vitrification degree, porosimetric distribution and interconnection of pore network) collected on representative samples belonging to the three petrographic fabric identified. Back-scattered images collected by scanning electron microscope highlight unvitified structure in samples belonging to Fabric A (a) and Fabric B (b) and vitrified structure in Fabric C (c). Mercury intrusion porosimetry results: (d, e, f) cumulative volume vs. pore radius plots and (g, h, i) intrusion-extrusion curves for representative samples of the three petrographic Fabric identified. The significance of the curves is discussed in the text.

Beside a slight variability in term of pore size distribution, samples belonging to Fabrics A (Figure 4 (d)) and B (Figure 4 (e)) exhibit a quite bimodal pore size distribution, with two main broad peaks centered at about 0.05 and 10  $\mu\text{m}$ , respectively. In detail, average pore radius of  $0.07\pm 0.04$   $\mu\text{m}$ , median pore diameter of  $5.56\pm 1.9$   $\mu\text{m}$  and modal pore diameter of  $0.8\pm 0.4$   $\mu\text{m}$  have been obtained for samples belonging to Fabric A, while values of  $0.06\pm 0.04$   $\mu\text{m}$  (average pore radius),  $2.15\pm 0.9$   $\mu\text{m}$  (median pore diameter) and  $0.8\pm 0.4$   $\mu\text{m}$  (modal pore diameter) have been obtained for Fabric B samples.

Otherwise, in sample of Fabric C, pores cover all the investigated ranges, with a peak around 10  $\mu\text{m}$  (Figure 4 (f)), average pore radius of 0.06  $\mu\text{m}$ , modal pore diameter of 3.67  $\mu\text{m}$  and median pore diameter about 0.4  $\mu\text{m}$ . Referring to porosity, value of about 20% has been measured in all analysed samples, with slightly greater values for samples of Fabric A (23%).

Additionally, the inspection of intrusion-extrusion curves allow to better understand the degree of interconnection of the pore network. For all studied samples the interconnection among pores is really

poor, as testified by the high hysteresis between the intrusion (increasing pressure) and extrusion (decreasing pressure) curves shown in Figure 4 (g, h, i) (the average values of total intruded volume are:  $0.13 \pm 0.03$  cm<sup>3</sup>/gin Fabric A samples,  $0.11 \pm 0.03$  cm<sup>3</sup>/gin Fabric B samples and  $0.11$  cm<sup>3</sup>/gin Fabric C ones).

#### 4. DISCUSSION

The archaeometric data collected on cooking ware fragments from Akrai allow us to obtain information on technology and provenance of studied potteries.

From petrographic point of view, three different typologies have been identified: the first one characterized by coarse grain texture and volcanic rock fragments as temper, the second one with medium-coarse grain texture and metamorphic rock inclusions and a third one characterized by volcanic glass inclusions and zeolites. This discrimination has been also confirmed by chemical data, for which both major and minor/trace elements allow to identify three different chemical groups. In particular, the three petrographic fabric are mainly differentiated by TiO<sub>2</sub>, Fe<sub>2</sub>O<sub>3</sub>, MgO and Na<sub>2</sub>O levels for major elements and Cr, Co, Ni and Rb for minor/trace ones. The really higher level of Fe<sub>2</sub>O<sub>3</sub>, MgO, Cr, Co and Ni exhibited by samples of Fabric C can be related to the composition of volcanic glass present as tempers in the clay paste.

The presence in Fabric A of mineralogical phases as anorthoclase, aegirine and aenigmatite can be considered a fingerprint of a specific cooking-ware class namely Pantelleria ware; the term is referred to a kitchen ware produced in Pantelleria from 1 B.C. to 6 A.D. (Schmidt, 2015). Referring to potteries belonging to Fabric B, they are characterized by petrographic features, in term of groundmass and inclusions, that exhibit a similarity with a well-known cooking-ware production active in Messina in Roman Age. Finally, for samples of Fabric C, petrographic features compatible with Sicilian productions from Lentini (Agodi *et al* 1998) have been observed.

On the basis of the aforementioned, in order to confirm the previously hypotheses on provenance, chemical composition of studied samples have been compared with reference data of Pantelleria (Montana *et al.* 2007), Messina (Barone *et al.* 2005b) and Lentini (Agodi *et al.* 1998) cooking-ware productions. The statistical treatment of chemical data (Figure 5) highlights a good agreement between petrographic observation and samples clusters, confirming the hypotheses of Pantelleria provenance for Fabric A samples and Messinian production for Fabric B ones; for samples belonging to Fabric C a similarity with Lentini production can be observed.

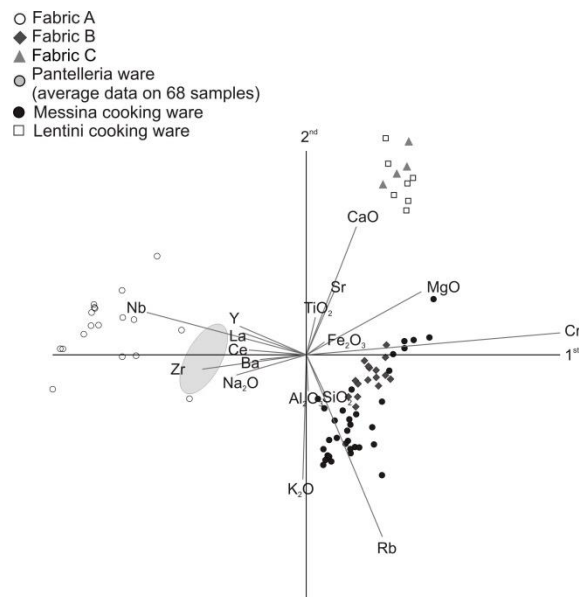


**Figure 5. Chemical composition of studied samples. Plot of recalculated data on LOI-free basis of the two principal components. Major elements: SiO<sub>2</sub>, Al<sub>2</sub>O<sub>3</sub>, TiO<sub>2</sub>, Fe<sub>2</sub>O<sub>3</sub>, CaO, MgO, Na<sub>2</sub>O, K<sub>2</sub>O; minor elements; Sr, Cr, Rb, Zr, Nb. Cooking wares samples and reference data from Pantelleria (Montana *et al.* 2007), Messina (Barone *et al.* 2005b) and Lentini (Agodi *et al.* 1998) are reported.**

Considering the technological aspects, information gained from groundmass birefringence, mineralogical phases and micro-morphological observations allow to estimate firing temperature, while porosimetric analyses allow to obtain additional manufacture parameters. In particular, in the case of Fabric A samples, the medium-high birefringence and the absence of vitrification suggest low firing temperature ( $T_{\max} \sim 800$  °C); however, the heterogeneous color of groundmass and the presence of hematite detected both by XRD patterns and micro-Raman spectra acquired on the matrix indicate possible irregular firing conditions with the development of high-temperature micro-domains; this observation could be supported also by the not uniform burnished surface of the vessels. Referring to samples belonging to Fabric B, the medium birefringence and the absence of vitrification structures suggest intermediate firing temperature ( $T_{\max}$  above 800 °C). Finally, for samples of Fabric C, the results obtained by petrographic, mineralogical and SEM analyses (*i.e.*, absence of birefringence, presence of Ca-silicates in mineralogical composition and vitrification of microstructure) suggest the achievement of high firing temperature ( $T_{\max} > 850$  °C). In addition, the presence of amorphous carbon detected by micro-Raman analyses could suggest the use of organic tempers in the clay paste and justify the black color of the groundmass, previously observed.

Parameters as firing temperature and vitrification degree have a great influence on porosity and pore

structure of ceramic materials. The overall of aforementioned features represents important factor in studying technological aspects of cooking ware, as they influence also the thermal proprieties of vessels (Tite *et al.* 2001; Wolf, 2002; Volzone and Zagorodny, 2014).

In fact, in low firing conditions the clay structure of ceramics is poor affected by mineralogical reactions and structural modifications and in these conditions the porosimetric features are usually characterized by a wide range of pore (polymodal/bimodal distribution) and relatively high porosity (Figure 6(a)). Otherwise, in condition of high firing temperature, the progressively vitrification and the bloating of the materials determine a collapse of small pores with a consequently unimodal distribution of pore size and a shift of median pore size towards higher values (Figure 6(b)). In general, the presence of wide size of unconnected pores, in association with a high concentration of tempers, allows to obtain more resistant materials against thermal shock (Arnold, 1998). It is quite clear, therefore, that the whole of the previous parameters is a good indicator of the manufacture features and technological quality of a ceramic production.

In view of the above, considering the firing temperatures estimated by petrographic observations, mineralogical data and micro-morphological observations, as well as the characteristics of studied sam-

ples in term of surface, groundmass, porosity, grain size and thickening of tempers, different manufacture features can be assessed for the three cooking ware productions identified. In detail, the homogeneity of groundmass, the abundance of inclusions (temper:groundmass ratio 30:70), the medium-low firing temperature esteemed ( $T_{max} > 800$  °C), the absence of vitrification, the wide range of pore size and the poor connected pore network, in association with the chemical composition, allow to establish a really specialized manufacture for samples from Messina (Fabric B), as confirmed by other researches that identified in this city several high expert workshops for the cooking-ware production (Coppolino, 2002). Similar observations can be inferred for Pantelleria ware production (Fabric A), for which the abundance of tempers (temper:groundmass ratio 40:60), the bimodal pore size distribution, the unconnected pore networks, the low firing temperature estimated ( $T_{max} \sim 800$  °C) and the absence of vitrification suggest good technological proprieties, as evidenced also by Montana *et al.* (2007). Otherwise, in the case of Lentini ware production (Fabric C), the higher firing temperature reached ( $T_{max} \sim 850$  °C), testified by the initial stage of vitrification observed by SEM investigations, in association with the unimodal pore size distribution measured by porosimetric analysis and the low temper:groundmass ratio, suggest a lower manufacture quality for these class of materials.

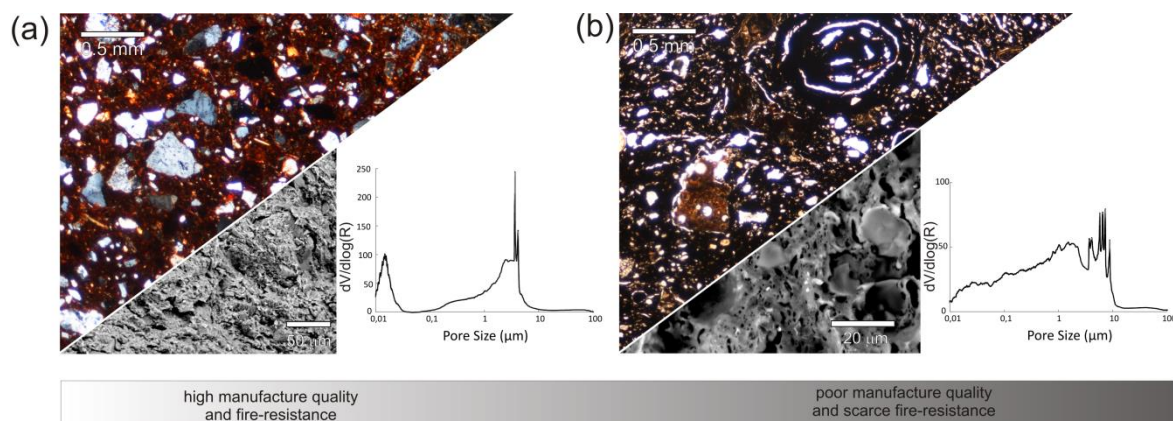


Figure 6. Schematic examples of (j) high cooking-ware manufacture (high concentration of tempers, absence of vitrification and polymodal pore size distribution) and (k) poor cooking-ware manufacture (low concentration of tempers, vitrified matrix and unimodal pore size distribution) on the basis of petrographic features, vitrification degree and pore size distribution.

## 5. CONCLUSIONS

The obtained results on cooking wares from Akrai define a complete scenario on the circulation and production of ceramic materials over the investigated time interval during which the Romanization of Sicily took place.

In detail, the presence of Pantelleria-ware and Messinian cooking pottery inform us about a mobili-

ty of goods from north-eastern Sicily and Pantelleria to the south-eastern area of the island. Moreover, the dating of the stratigraphic units suggests changes in circulation of cooking-ware over the time. In fact, samples recognized as Pantelleria-ware (pots as CP1, CP2, CP14 and lids as L1, L2, L3) were recovered in a stratigraphic interval ranging from end of the 1B.C. to 6A.D., corresponding to apex of chronological dif-



fusion of Pantellerian Ware and testifying a wide diffusion of this type in Sicily (Barone *et al.* 2010); otherwise, cooking-wares from Messina (pans P1, casseroles CP6, pots CP11 and lids L2) appear only in the archaeological layers dated to later periods. Finally, the presence of a small number of specimens of cooking-ware characterized by petrographic and chemical features compatible with the Lentini cooking-ware allow to suppose importation trade from this nearby town, maybe not really advanced due to the poor-quality of the production.

In conclusion, even if archaeologists suppose a local production named Akrai Cooking Ware by Wicenciak (Wicenciak, 2015), the archaeometric evidences and the absence of findings referring to pottery kiln strongly suggest that all the cooking-wares in Akrai were imported from other production centers. Additionally, the change in artifacts supplying in the investigated time lap opens interesting questions about the cultural and political transformation in the site during the Romanization process.

## ACKNOWLEDGEMENTS

The excavations and archaeometric analysis were done with financial aid of the Polish National Science Centre (UMO-2011/03/B/HS3/00567) and Polish Ministry of Science and Higher Education (4815/E-343/SPUB/2012/3 and 4815/E-343/SPUB/2013/3-1). The pottery was elaborated and studied from the typological standpoint by Prof. Jolanta Młynarczyk, Dr Urszula Wicenciak, Dr Krzysztof Domzalski, Monika Więch M.A and Marta Fituła.

## REFERENCES

- Agodi, S., Frasca, M., Mazzoleni, P., Pezzino, A. (1998) Indagine statistica sulla variabilità chimica delle ceramiche ellenistiche di Catane, Lentinoi e Syracusai (Sicilia Orientale), in *V Giornata le Scienze della Terra e l'Archeometria* (eds. C. D'Amico, C. Tampellini), 11-14, Patron Editore, Bologna.
- Aitchison, J. (1986) *The statistics analysis of compositional data* London, UK, Chapman and Hall.
- Arnold, D.E. (1998) *Ceramic Theory and Cultural Process (New studies in Archeology)*, University of Cambridge, New York.
- Aquila, E., Barone, G., Mazzoleni, P. and Ingoglia, C. (2012) Petrographic and chemical characterisation of fine ware from three Archaic and Hellenistic kilns in Gela, Sicily, *Journal of Cultural Heritage*, vol. 13, pp. 442-447.
- Barone, G., Lo Giudice, A., Mazzoleni, P. and Pezzino, A. (2005a) Chemical characterization and statistical multivariate analysis of ancient pottery from Messina, Catania, Lentini and Siracusa (Sicily), *Archaeometry*, vol.47(4), pp. 745-762.
- Barone, G., Ioppolo, S., Majolino, D., Branca, C., Sannino, L., Spagnolo, G., Tigano, G. (2005b) Archaeometric analyses on pottery from archaeological excavation in Messina (Sicily, Italy) from the Greek archaic to the Medieval age, *Periodico di Mineralogia*, vol. 74, pp. 11-41.
- Barone, G., Crupi V., Majolino, D., Mazzoleni, P., Teixeira, J., Venuti, V. (2009) Small angle neutron scattering as fingerprinting of ancient potteries from Sicily Southern Italy, *Journal Appl. Phys*, vol. 106, 054904.
- Barone, G., Belfiore, C.M., Mazzoleni, P., Pezzino, A., Viccaro, M. (2010) A volcanic inclusions based approach for provenance studies of archaeological ceramics: application to pottery from southern Italy, *Journal Archaeological Science*, vol. 37, pp. 713-726.
- Barone, G., Mazzoleni, P., Spagnolo, G., Aquilia, E. (2012) The transport amphorae of Gela: a multidisciplinary study on provenance and technological aspects, *Journal of Archaeological Science*, vol. 39, pp. 11-22.
- Barbera, G., Barone, G., Crupi, V., Longo, F., Maisano, G., Majolino, D., Mazzoleni, P., Teixeira, J., Venuti, V. (2013) Small angle neutron scattering study of ancient pottery from Syracuse (Sicily, Southern Italy), *Journal Archaeological Science*, vol. 40, pp. 983-991.
- Barone, G., Mazzoleni, P., Aquilia, E., Barbera, G., 2014, The Hellenistic and Roman Syracuse (Sicily) fine pottery production explored by chemical and petrographic analysis, *Archaeometry*, vol. 56, pp. 70-87.
- Chowaniec, R., 2015, The Sicilian world after the Punic Wars: the Greek colony in a new reality, in *Interdisciplinary Perspectives on Colonisation, Maritime Interaction and European Cultural Integration* (eds. H. Glørstad, L. Melheim and Z. Glørstad), Sheffield.
- Chowaniec, R., 2013, Ancient Akrai in the light of new researches. Non-invasive researches in Palazzolo Acreide, south-eastern Sicily, in *SOMA 2012 Identity and Connectivity, Proceedings of the 16th Sympo-*

- sium on *Mediterranean Archaeology* (eds. L. Bombardieri, A. D'Agostino, G. Guarducci, V. Orsi and S. Valentini), 965-971, Oxford.
- Coppolino, P., 2002, La ceramica comune "da fuoco" a Messina tra il VII e IV sec. a.C.: una nota preliminare, In *Da Zancle a Messina: un percorso archeologico attraverso gli scavi* (eds. G.M. Bacci and G. Tigano), 47-58, Sicania, Messina.
- Cultrone, G., Rodriguez-Navarro, C., Sebastian, E., Cazalla, O., DelaTorre, M.J., 2001, Carbonate and silicate phase reactions during ceramic firing, *European Journal of Mineralogy*, vol. 13, pp. 621-634.
- Maggetti, M., 1982, Phase analysis and its significance for technology and origin in *Archeological Ceramics* (eds. J.S. Olin and A.D. Franklin), 121-133, Smithsonian Inst. Press, Washington.
- Maniatis, Y., Tite, M.S., 1981, Technological Examination of Neolithic-Bronze Age Pottery from Central and Southeast Europe and from the Near East, *Journal of Archaeological Science*, vol. 8, pp. 59-76.
- Montana, G., Fabbri, B., Santoro, S., Gualtieri, S., Iliopoulos, I., Guiducci, G., Mini, S., 2007, Pantellerian Ware: A Comprehensive Archaeometric Review, *Archaeometry*, vol. 49, pp. 455-481.
- Munsell Color, 2000, *Munsell soil color chart*, Gretag Macbeth, New Windsor.
- Riccardi, M.P., Messiga, B., Duminuco, P., 1999, An approach to the dynamics of clay firing, *Applied Clay Science*, vol. 15, pp. 393-409.
- Schmidt, K., 2015, Fabrics of Pantelleria (Cossyra), in FACEM <http://www.facem.at/project-papers.php>. Last access January.
- Thió-Henestrosa, S. and Martín-Fernández, J. A., 2005, Dealing with compositional data: the freeware CoDaPack, *Mathematical Geology*, vol. 37, pp. 773-793.
- Tite, M.S., Kilikoglou, V., Vekinis, G., 2001, Strength, Toughness and Thermal Shock Resistance of Ancient Ceramics, and Their Influence On Technological Choice, *Archaeometry*, vol. 43, pp. 301-324.
- Wicenciak, U., 2015, Kitchen and Cooking wares in Akrai. First remarks, in *Unveiling the past of an ancient town. Akrai/Acrea in south-eastern Sicily* (eds. R. Chowanec) Warsaw.
- Whitbread, I. K., 1995, Greek transport amphorae: a petrological and archaeological study, in *Fitch Laboratory Occasional Paper*, 4, British School at Athens, Athens.
- Wolf, S., 2002, Estimation of the production parameters of very large medieval bricks from St. Urban, Switzerland, *Archaeometry*, vol. 44, pp. 37-65.
- Volzone, C., Zagorodny, N., 2014, Mercury intrusion porosimetry (MIP) study of archaeological pottery from Hualfin Valley, Catamarca, Argentina, *Applied Clay Science*, vol. 91-92, pp. 12-15.